Available online at www.sciencedirect.com
ScienceDirect
Journal of Photochemistry and Photobiology A: Chemistry 192 (2007) 75–83
Journal of Photochemistry and Photobiology A:Chemistry
www.elsevier.com/locate/jphotochem

Spironaphtoxazines produced from crown-containing dihydroisoquinolines: Synthesis and spectroscopic study of cation-dependent photochromism

Valeri V. Korolev [a], Dmitry Yu. Vorobyev [a], Evgeni M. Glebov [a,*], Vjacheslav P. Grivin [a], Victor F. Plyusnin [a], Alexander V. Koshkin [b], Olga A. Fedorova [b], Sergei P. Gromov [b], Mikhail V. Alfimov [b], Yuri V. Shklyaev [c], Tatyana S. Vshivkova [c], Yuliya S. Rozhkova [c], Alexander G. Tolstikov [c], Vladimir V. Lokshin [d], Andre Samat [d]

[a] *Institute of Chemical Kinetics and Combustion SB RAS, Novosibirsk 630090, Russian Federation*
[b] *Photochemistry Center of Russian Academy of Sciences, Moscow 11742, Russian Federation*
[c] *Institute of Technical Chemistry UB RAS, Perm 614990, Russian Federation*
[d] *Faculté des Sciences de Luminy, Université de la Méditerranée, UMR 6114 CNRS, Marseille, France*

Received 5 December 2006; received in revised form 13 March 2007; accepted 2 May 2007
Available online 6 May 2007

Abstract

Synthesis and photochromic properties of a novel spironaphtoxazine (SNO) obtained from a crown-containing dihydroisoquinoline are described. The comparison of spectral and kinetic properties with that of a crown free SNO is performed. For a crown-containing SNO, the complex formation with alkaline earth metal cations occurs both for spiro (S) and merocyanine (M) forms of the molecule. For the cations of large size (for instance, Ba^{2+}) the formation of sandwich complex was found. For a crown free SNO, only M-form complex with metal cation is possible. In all cases, the complex formation affects both on the position of the M-form absorption maximum and the M-form characteristic lifetime.

Keywords: Spironaphthoxazine; Dihydroisoquinoline; 15-Crown-5-ether; Complex formation; Electrocyclic transformation; Photochromism

1. Introduction

Crown ethers have found applications in many areas due to their ability to recognize metal ions. Among other things, the photochromic properties of compounds containing crown-ether or calyx [4] arene moieties could be controlled by metal cations [1–27]. The binding of cations by ionophoric fragments could lead to the change of such properties of photochromes as photostability, sensitivity and width of operative optical region.

Osa and co-workers [1] synthesized spirobenzopyran derivatives bearing benzo-15-crown-5 and examined their photoresponsive cation binding ability. Inouye et al. [2] demonstrated the influence of alkali metal cations on the spectral properties of an azacrown-containing spiropyran. In development of the approach [1,2], the influence of metal cations on the photochromic properties was reported for different crown-containing spiropyrans [3–10], spirooxazines [11–21], 2-styrylbenzothiazoles [22,23], and chromenes [24,25]. As an example, spirobenzopyran derivatives with a monoazacrown moiety at the 8 position demonstrate cation-dependent photochromic properties. E.g., in the presence of Li^+ ions the merocyanine M-form is stabilized [4]. Its lifetime increases in an order of magnitude. The reason of the stabilization is the formation of complexes between a metal cation and the M-form of crown-containing spiropyrane [4].

Spirooxazines are considered as more reliable photochromic control systems than spiropyrans due to excellent light-fatigue resistance [28]. The effect of metal ions on the photochromic properties of spirooxazines could be very significant. As an example, incorporation of monoaza-12-crown-4 group in the 5′ position of a spironaphtoxazine derivatives leads to the dramatic dependence of M-form lifetime on the concentration of Li^+ ions [12]. The observed stabilization effect was as large as two orders of magnitude [12].

* Corresponding author. Tel.: +7 383 3332385; fax: +7 383 3342350.
E-mail address: glebov@ns.kinetics.nsc.ru (E.M. Glebov).

1010-6030/$ – see front matter © 2007 Elsevier B.V. All rights reserved.
doi:10.1016/j.jphotochem.2007.05.006

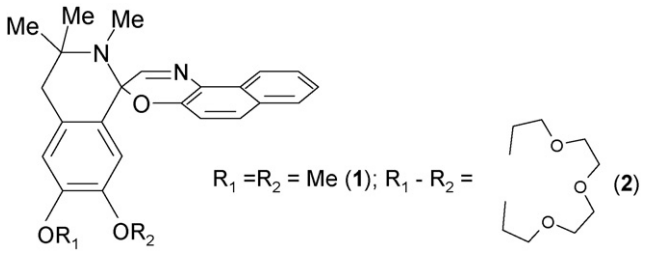

Scheme 1.

This work is in the scope of authors efforts mounted to the development of the spironaphtoxazine based photochromic systems most sensitive to the presence of metal cations [13–18,26,27]. In [14,15], a crown-containing fragment was incorporated to the oxazine moiety of spironaphtoxazine (SNO) via a flexible spacer. Several types of complexes between crown-containing SNO and metal ions were found. Its stability constants demonstrated the dependence on the size of metal cations. When metal ion is smaller than the radius of the cavity in the crown ether ring, a so called anion-capped complex forms due to the Coulomb interaction between the partly charged oxygen atom of the M-form and the ion disposed in the cavity. In this case, the rate constant of the M → S reaction could decrease in an order of magnitude [15]. For the cations which are bigger than the crown ether cavity, the stabilization effect is much smaller [15]. It was found that the rigid spacer structure prevents the formation of anion capped complex, and the effect of metal ions on the M-form stability is much smaller than in the case of a flexible spacer [13]. For SNO conjugated with azacrown ether moieties at the 6′-position of the oxazine fragment, the effect of metal cations on the spectra of both S-form and M-form was observed [16]. Two probable sites of the complex formation are possible: the crown ether centre and the M-form oxygen atom in the oxazine moiety of SNO. The correspondence between the crown cavity and the metal cation sizes were found to be important for the effective binding.

In the present paper, the synthesis and photochromic properties of SNO with a crown-containing fragment in the isoquinoline part of the molecule (SNO **2** in Scheme 1) is reported. For comparison, SNO **1** which has no crown ether moiety was used (Scheme 1). Further in the text spiro and merocyanine forms of SNO **1** and SNO **2** are marked as S-**1**, S-**2**, M-**1** and M-**2** correspondingly. For the study of complex formation between SNO and metal cations, Mg^{2+} and Ba^{2+} were chosen. The ionic radii of these ions are 0.72 and 1.36 Å correspondingly [29]. Radius of 15-crown-5-ether is 0.85 Å [30]. Thus, Mg^{2+} cation fits well to the size of the crown ether ring, and its position in the centre of the cavity is expected. For Ba^{2+} cation the complexation should take place outside of the cavity, probably, leading to the formation of sandwich complexes.

2. Experimental

2.1. Materials

$Mg(ClO_4)_2$ and $Ba(ClO_4)_2$ (Aldrich) were used as the sources of Mg^{2+} and Ba^{2+} ions. Spectrophotometric grade acetonitrile (Aldrich), was used as a solvent.

2.2. NMR study

^{1}H NMR spectra were recorded on a Bruker DRX500 instrument (500.13 MHz) for solution in CD_3CN, the solvent being used as the internal reference 1.96 ppm for ^{1}H; for solution in $CDCl_3$, the solvent being used as the internal reference 7.27 ppm for ^{1}H.

2.3. Synthesis of the SNO

The widely applied procedures for the synthesis of the spirooxazines [31] consisting in the condensation of nitrogen-containing heterocycles with hydroxynitroso compounds was used for the obtaining of the compounds SNO **1** and SNO **2** (1 and 2 in Scheme 2). The pathway of the synthesis is shown in Scheme 2. The 1,3,3-trimethyl-3,4-dihydroisoquinolines **3**, **4** were prepared as described in [32]. The isoquinoline salts **5**, **6** [32] were prepared by the interaction of **3**, **4** [32] with methyl iodide.

The mixture of the 0.5 mmol **5** or **6**, 0.5 mmol 1-nitroso-2-naphthol and 0.6 mmol Et_3N was heated in 15 ml MeOH during 2 h in inert atmosphere. After finishing the reaction, the product was purified by coloumn chromotography (Silicagel 60, eluent cyclohexane/ethyl ether from 100:1 up to 1:1).

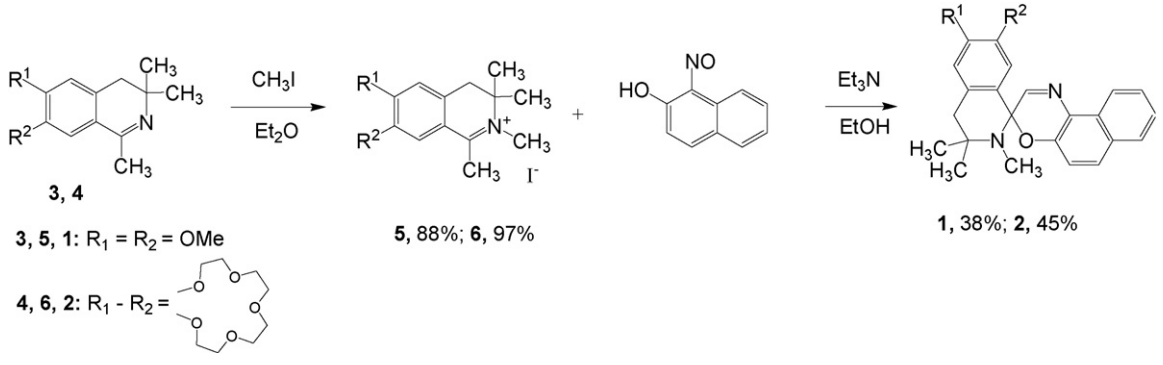

Scheme 2.

*2.4. 3,4-Dihydro-2,3,3-trimethyl-6,7-dimethoxyspiro-[isoquinolino-1,3′-[3H]napht[2,1-b][1,4]oxazine] (**1**)*

45%, yellow oil, NMR ^{1}H ($CHCl_3$-d_1, δ, mp, J, Hz.): 1.26 (s, 3H, CH_3); 1.31 (s, 3H, CH_3), 2.22 (s, 3H, N-CH_3), 2.58 (d, 1H, H-4a, J = 15.6), 2.93 (d, 1H, H-4b, J = 15.6), 3.65 (s, 3H, CH_3O), 3.89 (s, 3H, CH_3O), 6.56 (s, 1H, H-5), 6.62 (s, 1H, H-8), 7.06 (d, 1H, H-5′, J = 8.9), 7.18 (s, 1H, H-2′) 7.38 (t-d, 1H, H-8′, J = 8.2, 8.1 и 1.3), 7.57 (t-d, 1H, H-9′, J = 8.2, 8.4 and 1.3), 7.71 (d, 1H, H-6′, J = 8.9), 7.79 (d, 1H, H-7′, J = 8.1), 8.59 (d, 1H, H-10′, J = 8.4). Elemental analysis: calc.: C, 74.60; H, 6.51; N, 6.96. $C_{25}H_{26}N_2O_3$; found: C, 74.72; H, 6.59; N, 6.89.

*2.5. 3,4,7,8,10,11,13,14,16,17-Decahydro-2,3,3-trimethylspiro[(6,9,12,15,18)penta-oxacyclopentadecyno-[2,3-g]isoquinolino-1,3′-[3H]napht[2,1-b][1,4]oxazine (**2**)*

38%, light-yellow oil. NMR ^{1}H ($CHCl_3$-d_1, δ, mp, J, Hz.): 1.24 (s, 3H, CH_3); 1.29 (s, 3H, CH_3), 2.21 (s, 3H, N-CH_3), 2.54 (d, 1H, H-4a, J = 15.6), 2.90 (d, 1H, H-4b, J = 15.6), 3.73 (m, 8H, 4 OCH_2), 3.90 (m, 4H, 2 OCH_2), 4.12 (m, 4H, 2 OCH_2), 6.53 (m, 1H, H-5), 6.60 (s, 1H, H-8), 7.04 (d, 1H, H-5′, J = 8.9), 7.16 (s, 1H, H-2′) 7.37 (t-d, 1H, H-8′, J = 8.1, 8.1 and 1.1), 7.56 (t-d, 1H, H-9′, J = 8.1, 8.2 and 1.1), 7.69 (d, 1H, H-6′, J = 8.9), 7.75 (d, 1H, H-7′, J = 8.1), 8.59 (d, 1H, H-10′, J = 8.2). Elemental analysis: calc.: C, 69.90; H, 6.81; N, 5.26. $C_{31}H_{36}N_2O_6$; found: C, 69.69; H, 6.89; N, 5.20.

*2.6. Synthesis of the complexes of SNO **2** with $Mg(ClO_4)_2$ and $Ba(ClO_4)_2$*

$Mg(ClO_4)_2$ (3 mg, 0.014 mmol) or $Ba(ClO_4)_2$ (2.3 mg, 0.007 mmol) and SNO **2** (7.4 mg, 0.014 mmol) were dissolved in 0.6 ml CD_3CN. The resulting complex (SNO **2**)·Mg^{2+} or (SNO **2**)$_2$·Ba^{2+} was used for NMR (see Fig. 6a and b) and ESI MASS investigation. The main peaks found in ESI MASS spectra are presented in Scheme 4.

2.7. Spectrocopic measurements

UV absorption spectra were recorded using a HP-8453 spectrophotometer (Hewlett Packard) with the characteristic time of recording ca. 2 s. High pressure mercury lamp with the set of glass filters was used as a light source for stationary photolysis. To measure rate constants of the M → S reactions of SNO with the characteristic time of several seconds, samples were irradiated in the cuvette box of the spectrophotometer. The irradiation was performed till the photostationary conditions (equilibrium between S and M-forms) were achieved, which was controlled by the absorption of M-form in the red spectral region. Then the irradiation was interrupted and the kinetic curves corresponding to the recovery of the system to the initial S-state were recorded.

Laser flash photolysis was also used to study the kinetics of the M → S reactions in the wide temporal range of 0.1 μs–10 s. Experiments were performed using a XeCl setup (308 nm, 20 ns, 20 mJ/pulse) described elsewhere [33]. For measurements in the temporal range shorter than 1 ms, a xenon lamp exploited in a pulsed mode was used as a source of probing light. For experiments performed in a longer temporal range, an incandescent lamp was used as a source of the probing light.

2.8. ESI-MASS measurements

Mass spectra were measured at an ionizing voltage of 2 kV in soft conditions by electrospray ionization mass spectrometry (ESI-MASS) with the use of the exact mass measurement method, employing an Agilent 1100 Series LC/MSD Trap mass spectrometer (400 μl/h; 10 V; 120 °C). The data were analyzed with the use of Molecular Weight Calculator, Version 6.37 (Matthwe Monroe).

3. Results and discussion

3.1. Complexes of SNO (S-form) with Mg^{2+} and Ba^{2+}

The spectrophotometric titration method, ^{1}H NMR and ESI-mass spectrometry were employed for analysis of the complexation processes. Both SNO **1** and SNO **2** in the absence of irradiation are completely in the spiro-form. The UV-spectra of colorless spiro-forms (S-**1**, S-**2**) in acetonitrile solutions are presented in Fig. 1. In the presence of alkaline earth metal cations the spectrum of crown free SNO **1** does not demonstrate any changes. For crown-containing SNO **2**, the addition of both Mg^{2+} and Ba^{2+} cations leads to the complex formation between SNO and metal ion.

The spectral evidence of the complex formation for the case of Mg^{2+} is shown in Fig. 2. The addition of ions in concentration comparable with the concentration of SNO **2** results in the decrease of the absorption intensity at 270–310 nm. The absence of the spectral changes in the case of SNO **1** makes it possible to

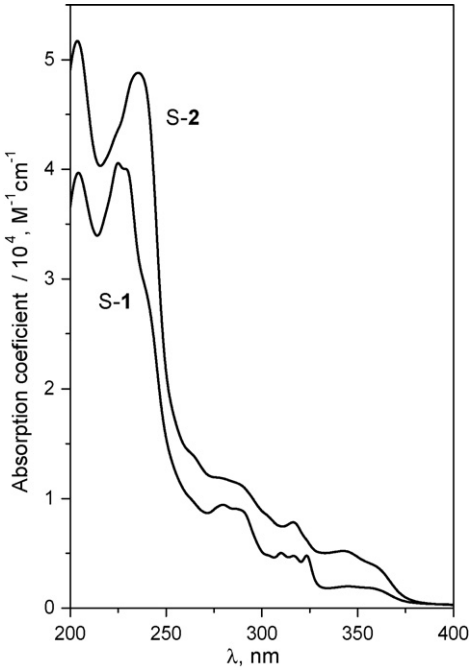

Fig. 1. UV spectra of S-form of SNO **1** (S-**1**) and **2** (S-**2**) in CH_3CN.

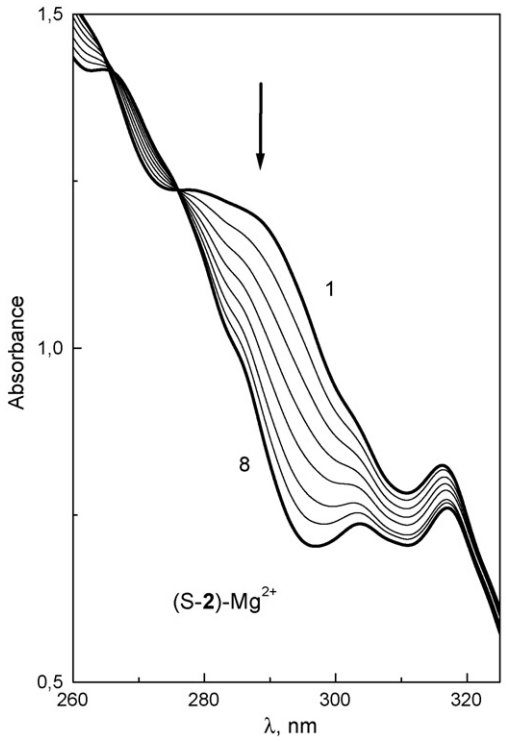

Fig. 2. Changes in the UV-spectrum of S-**2** (1×10^{-4} M) in the presence of Mg^{2+}. Temperature 298 K, cuvette 1 cm, solvent—CH_3CN. Curves 1–8 denote to $[Mg^{2+}]/[(S\text{-}\mathbf{2})]$ ratio 0; 0.17; 0.33; 0.5; 0.66; 0.84; 1.0; 1.2.

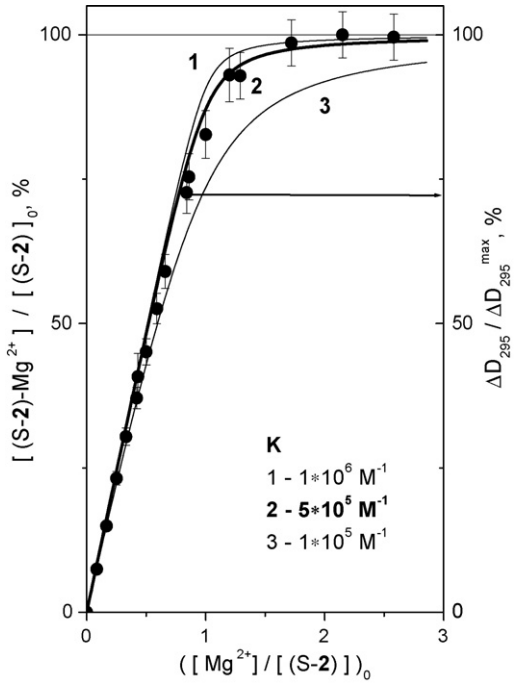

Fig. 3. Determination of composition and equilibrium constant of the (S-**2**)-Mg^{2+} complex. Relative changes in absorption at 295 nm (dots, right axis) and calculated values of the (S-**2**)-Mg^{2+} complex percentage (left axis) vs. $[Mg^{2+}]/[(S\text{-}\mathbf{2})]$ ratio. Curves 1–3 denote to equilibrium constants 1×10^6; 5×10^5; 1×10^5 M^{-1}.

conclude that the complex between S-**2** and Mg^{2+} forms due to coordination of the metal ion with the crown ether moiety. The conservation of the isosbestic points (266 and 276 nm, Fig. 2) supports an assumption that only two forms containing SNO **2** coexist in the solution. It allows one to use UV spectra to determine the composition of the complex and to estimate the equilibrium constant.

It is essential to assume that the change in absorption intensity in the characteristic spectral region (270–310 nm) is proportional to the percentage of the complex. The absorption at 295 nm (Fig. 2) was chosen to determine the composition of the complex by the method of molar ratios [34]. The molar ratios plot shown in Fig. 3 makes it evident that the composition of the (S-**2**)-Mg^{2+} complex is 1:1. It corresponds to the position of the metal ion inside the crown ether cavity. The proposed composition of the complex is shown in Scheme 3.

When Ba^{2+} cations are added to the solution of SNO **2**, the changes in the UV spectra (Fig. 4) are similar to those for Mg^{2+} cations. Isosbestic points at 247.5 and 349 nm are conserved, which allows one to determine the composition of the complex. The molar ratios plot (Fig. 5) demonstrates that the $[(S\text{-}\mathbf{2})]/[Ba^{2+}]$ ratio is equal to 2. The resulted $(S\text{-}\mathbf{2})_2$-Ba^{2+} complex was proposed to have the sandwich structure (Scheme 3), in accordance with the ratio of the sizes of metal cation and crown ether cavity.

The equilibrium constants of the complexes (S-**2**)-Mg^{2+} and $(S\text{-}\mathbf{2})_2$-Ba^{2+} were determined by the comparison of experimental and calculated dependencies of the relative concentrations of complexes via initial $[Met^{2+}]/[(S\text{-}\mathbf{2})]$ ratios. Fig. 3 demon-

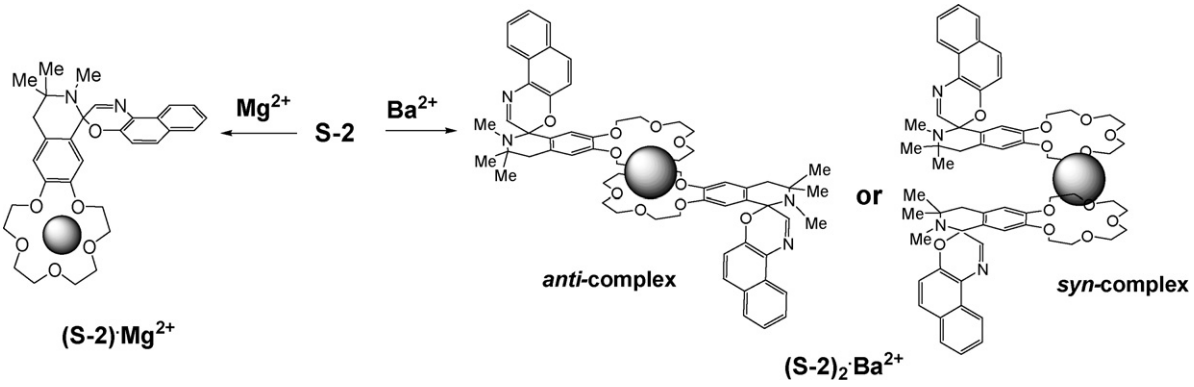

Scheme 3.

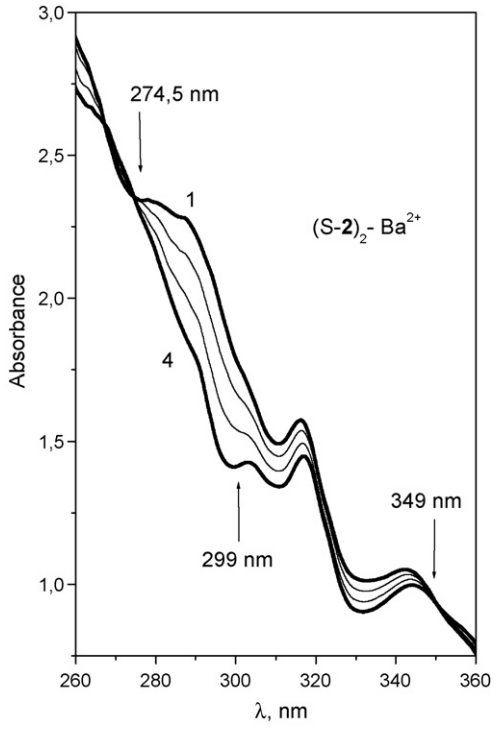

Fig. 4. Changes in the UV-spectrum of S-**2** (2×10^{-4} M) in the presence of Ba^{2+}. Temperature 298 K, cuvette 1 cm, solvent – CH_3CN. Curves 1–4 denote to $[Ba^{2+}]/[(S\text{-}\mathbf{2})]$ ratio 0; 0.16; 0.33; 0.66.

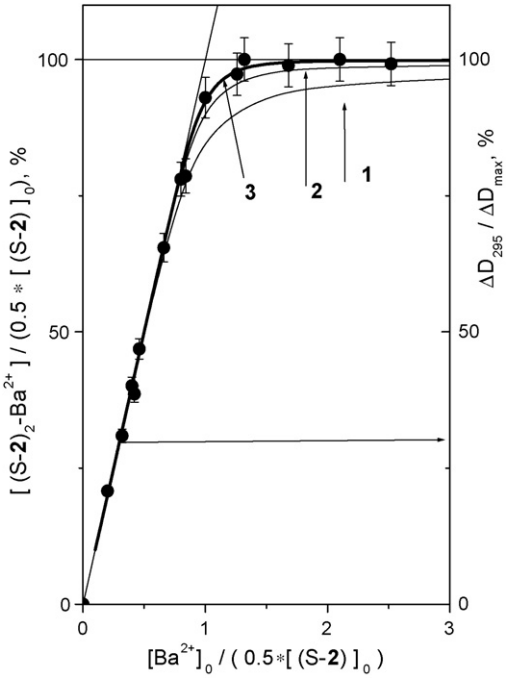

Fig. 5. Determination of composition and equilibrium constant of the (S-**2**) complex with Ba^{2+}. Relative change in absorption at 295 nm (dots, right axis) and calculated values of the $(S\text{-}\mathbf{2})_2$-Ba^{2+} complex percentage (left axis) vs. $[Ba^{2+}]/[(S\text{-}\mathbf{2})]$ ratio. Curves 1–3 denote to equilibrium constants 1×10^{10}; 5×10^{11}; 1×10^{12} M^{-2}.

Table 1
Equilibrium constants of SNO complexes with metal cations

Complex	K_{eq}
(S-**2**)-Mg^{2+}	5×10^5 M^{-1}
$(S\text{-}\mathbf{2})_2$-Ba^{2+}	$>1 \times 10^{12}$ M^{-2}
(M-**1**)-Ba^{2+}	1.5×10^3 M^{-1}
(M-**2**)-$(Mg^{2+})_2$	3×10^3 M^{-1} [a]

[a] Stability constant for (M-**2**)·$(Mg^{2+})_2$ complex is determined as $K_{eq} = [(\text{M-}\mathbf{2})(Mg^{2+})_2]/[Mg^{2+}][(\text{M-}\mathbf{2})Mg^{2+}]$.

strates this procedure for (S-**2**)-Mg^{2+} complex. Dots with error bars (right axes) represent the experimental relative changes in absorption at a characteristic wavelength (295 nm). Full lines 1, 2 and 3 (left axes) represent the calculated relative content of the complex for different values of the equilibrium constant. The experimental curve (Fig. 3) is satisfactorily fitted with the calculated curve corresponding to the value of $K_{eq} = 5 \times 10^5$ M^{-1}. All the equilibrium constants (for both S and M-forms of SNO) are listed in Table 1.

The procedure of determination of the equilibrium constant for $(S\text{-}\mathbf{2})_2$-Ba^{2+} complex is shown in Fig. 5. The stoichiometry of the complex (ratio $[(S\text{-}\mathbf{2})]/[Ba^{2+}] = 2$) was taken into account. In this case, the equilibrium constant is high, and all the metal cations added to (S-**2**) solution are bound till to the almost stoiciometric conditions. It allows one to obtain only an upper estimation for the equilibrium constant: $K_{eq} > 1 \times 10^{12}$ M^{-2}.

An addition of Mg^{2+} and Ba^{2+} cations to a solution of SNO **1** does not cause any changes in ^1H NMR-spectrum. In the case on crown-containing SNO **2**, the ^1H NMR-spectrum in MeCN-d_3 changes when metal cations are added (Fig. 6). Changes in the position of the crown ether proton signals (Fig. 6a) and aromatic proton signals (Fig. 6b) observed in ^1H NMR-spectra of SNO **2** in the presence of Mg^{2+} and Ba^{2+} cations are shown in Fig. 6. The influence of Mg^{2+} cations on the crown ether part of SNO **2** in NMR spectrum is substantially large in comparison with Ba^{2+} influnece. The difference is explained by the different types of formed complexes. Thus, Mg^{2+} is located in crown ether cavity due to good correspondence of the cation radii to the size of crown ether. The formation of Mg^{2+} inclusion complex causes the pronounced changes in chemical shifts of protons of benzocrown ether fragment. In the case of Ba^{2+} sandwich complex was found from optical experiments. The influence of metal cations is spreded between two crown ether moieties what decreases the effect of metal cations on spirocompound. The shifts of proton signal positions of SNO **2** in presence of Ba^{2+} cations are not so remarkable. The isoquinoline and oxazine fragments are near perpendicular to each other in the molecule. This accounts for spatial limitation of the complex formation; there are no changes of oxazine proton signal positions (H-2′, H-5′, H-6′, H-7′, H-8′, H-9′, H-10′).

The two possible structures for sandwich complexes *syn* and *anti* can be suggested (Scheme 3). In the *syn*-complex the mutual desposition of aromatic fragments should lead to the appearance of the anisotropic effect produced by ring-current magnetic field. The anisotropic effect is accompained by the upfield shifts of proton signals (namely, of 4-a and 4-b protons and, probably,

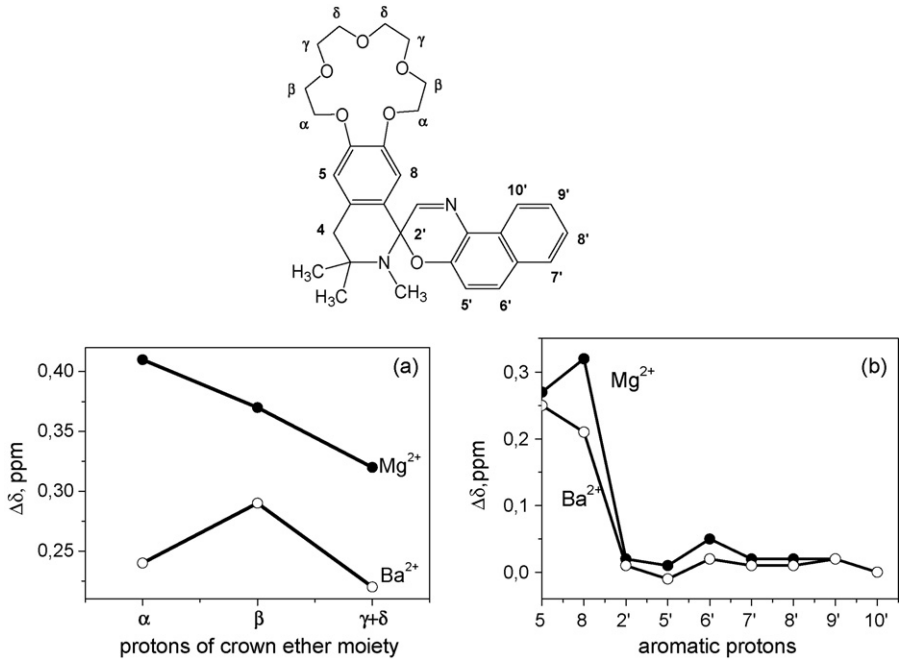

Fig. 6. Changes of the chemical shifts ($\Delta\delta = \delta_{complex} - \delta_{ligand}$, ppm) observed in ^{1}H NMR spectra of ligand SNO **2** in the presence of $Mg(ClO_4)_2$ and $Ba(ClO_4)_2$ in CD_3CN, ratio Mg/L = 1/1; Ba/L = 1/0.5; C_L—5×10^{-4} M/L.

of CH_3 groups protons). This fact has not been found in NMR experiments. Thus, the *syn*-complex structure could be excluded. The sandwich complex could exist as *anti*-isomer. Another possibility is a fast rotation of the two S-2 moieties. This rotation should be faster as the corresponding NMR time scale (>50 Hz).

The electrospray ionization mass spectrometry (ESI-MASS) provides direct and straightforward access to the accurate determination of complex composition in MeCN solution at different ligand/metal cation ratio. It is important to note that for comparative analysis the same concentration of complexes upon both UV- and ESI-MASS-analysis were used. Electrospray full scan spectra in the range *m*/*z* 100–1000 were obtained by infusion at 1 ml/min of a solution of each complex dissolved in pure acetonitrile. The full-scan spectra of SNO **2** complexes with metal cations in the positive ion mode are shown in Fig. 7a and b. Concluded from Fig. 7a, the signals at the mass-to-charge ratio *m*/*z* 655.1, 754.0, 881.0 correspond to the dominant complexes with the structure [(S-**2**)·$Mg(ClO_4)^+$], [(M-**2**)·$Mg(ClO_4)_2$] and [(M-**2**)·$Mg(ClO_4)^+$·$Mg(ClO_4)_2$] presented in solution. The structures of complexes proposed from ESI-MASS analysis are presented in Scheme 4. Thus, in course of ESI-MASS analysis complex S-**2** with Mg^{2+} transformed to open form which stabilized by coordi-

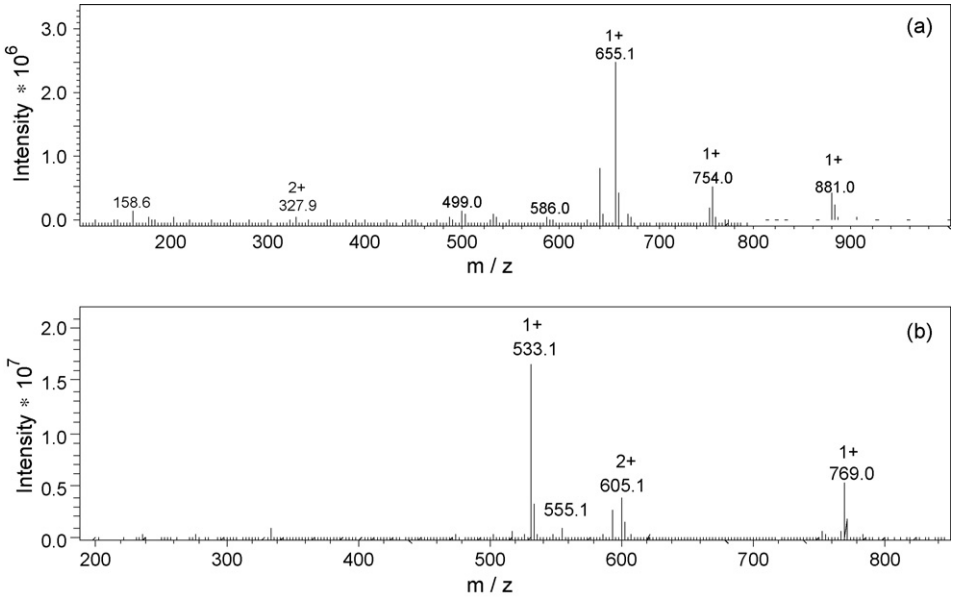

Fig. 7. ESI mass spectrum of SNO **2** (2×10^{-4} M) in the presence of metal ions: (a) $Mg(ClO_4)_2$ (2×10^{-4} M); (b) $Ba(ClO_4)_2$ (2×10^{-4} M).

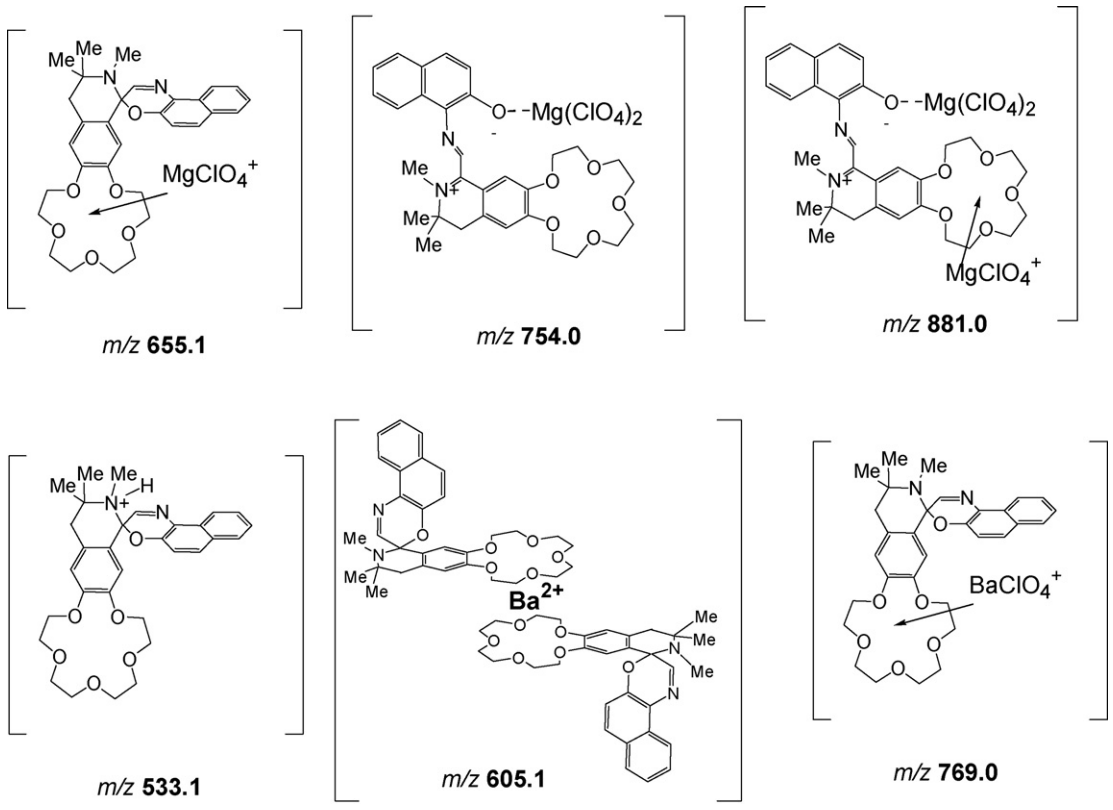

Scheme 4.

nation of Mg^{2+} with merocyanine oxygen atom. In the spectrum Fig. 7b the ions at *m*/*z* 605.1 and at *m*/*z* 769.0 are attributed to the sandwich complex [(S-**2**)$_2$·Ba^{2+}] and perchlorate adduct [(S-**2**)·Ba ClO_4]$^+$. The mass-spectrum results on complex formation of S-**2** with Mg^{2+} and Ba^{2+} cations demonstrate fully coincidence with those obtained by UV-spectroscopy. These findings support that electrospray reflects qualitatively the supramolecular species present in solution.

3.2. Photochromic properties of SNO

The irradiation of spiro-forms of both SNO **1** and SNO **2** leads to the formation of merocyanine (M) form (Scheme 5), which demonstrates an intensive visible absorption band in the region at 600 nm.

The kinetic curves of M → S transitions are exponential with the characteristic lifetimes of several seconds at a room temperature. Fig. 8 shows an example of kinetic curves (Fig. 8a)

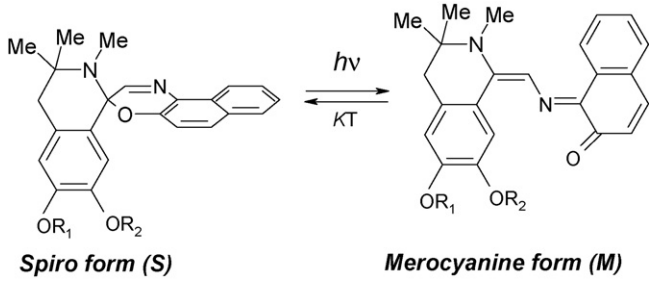

Scheme 5.

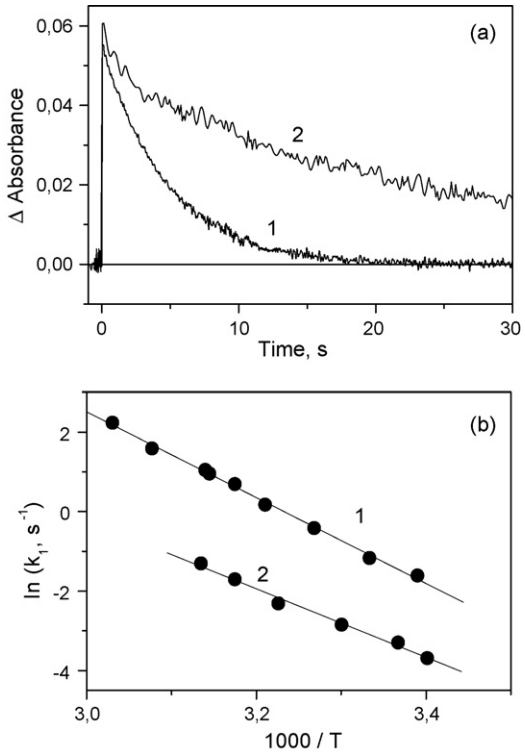

Fig. 8. Laser flash photolysis (308 nm) of SNO **1** (2×10^{-4} M) in the absence of metal ions (curves 1) and in the presence of 0.053 M Ba^{2+} (curves 2). (a) Kinetic curves (temperature 297 K, cuvette 0.5 cm, recording at 600 nm); (b) Arrenius plots.

and Arrenius plots (Fig. 8b) for M → S reactions. The values of activation energies are always in the range of 65–90 kJ/mol, which is typical for all the SNO [35]. The spectral and kinetic properties of M-form both in the absence and in the presence of metal ions are listed in Table 2.

3.3. Metal cation effect on the properties of M-form of SNO 1,2

When metal cations are added to the solutions of SNO **2** in concentration comparable with the concentration of spirooxazine, no changes in the spectra of M-form occur. However, it is evident from Table 2 that the stability of SNO **2** M-form decreases in the presence of both Mg^{2+} and Ba^{2+}. Rate constants of M → S transitions for (M-**2**)-Mg^{2+} and (M-**2**)$_2$-Ba^{2+} complexes are 16 and 4 times higher than for free M-**2** (Table 2). The possible reason of the decrease in the stability of merocyanine form is the Coulomb repulsion between the metal cation and the partial *positive* charge of M-form ($N^{\delta+}$), which is located on the nitrogen atom of the isoquinoline ring (Scheme 1). For the sandwich (M-**2**)$_2$-Ba^{2+} complex the effect of destabilization is sufficiently less than for (M-**2**)-Mg^{2+}, where the metal cation is located inside the crown ether cavity. It is possible that for a sandwich structure like (M-**2**)$_2$-Ba^{2+} the screening of the Coulomb interaction between the metal cation and $N^{\delta+}$ is more sufficient than for the (M-**2**)-Mg^{2+} structure.

When metal cations are taken in large excess (ca. 100 times), both SNO **1** and SNO **2** demonstrate the stabilization of the M-form. This effect compensates and surpasses the initial increase in M → S rate constants. For crown free SNO **1**, the effect of M-form stabilization due to Ba^{2+} cations is about an order of magnitude in comparison with free spironaphtoxazine (Table 2). For crown-containing SNO **2**, the effect is not so large, but also sufficient.

The stabilization of M-form is accompanied by a hypsochromic shift of the maximum of M-form absorption band (Fig. 9a). This effect was observed both for SNO **1** and SNO **2**. The stabilization of M-form of SNO **1** could be explained by the cation binding by an oxygen atom of the oxazine moiety of merocyanine (this atom carries a partial negative charge). As a result (M-**1**)-Ba^{2+} complex is formed (Scheme 3). Assuming the relative shift of the M-form absorption maximum linearly depends on the fraction of complexed M-**1**, the stability constant of (M-**1**)-Ba^{2+} was estimated. The procedure of estimating the stability constant is demonstrated by Fig. 9b. The experimental dependence of the relative shift of the absorption band maximum on the relative content of metal cations (dots in Fig. 9b) is satisfactorily fitted by the calculated dependence of the complex content with the equilibrium constant 1.5×10^3 M^{-1} (full lines in Fig. 9b and Table 2).

Table 2
Properties of M-form of SNO and their complexes with metal ions

Complex (ligand to metal ratio)	λ_M^{max} (nm)	$k_{M\rightarrow S}$ (298 K) (s^{-1})	E_{act} (kJ/mol)
Free M-**1**	607	0.26	90 ± 6
(M-**1**)-Ba^{2+} (1:265)	581	0.037	72 ± 7
Free M-**2**	607.5	0.28	87 ± 6
(M-**2**)$_2$-Ba^{2+} (1:0.52)	607.5	0.99	–
(M-**2**)$_2$-Ba^{2+} (1:1.2)	607.5	1.2	–
(M-**2**)-(Ba^{2+})$_2$ (1:500)[a]	592	0.17	81 ± 9
(M-**2**)-Mg^{2+} (1:1.22)	607.5	4.35	–
(M-**2**)-(Mg^{2+})$_2$ (1:157)	572	0.17	69 ± 6

[a] For this complex another structures are also possible, see text.

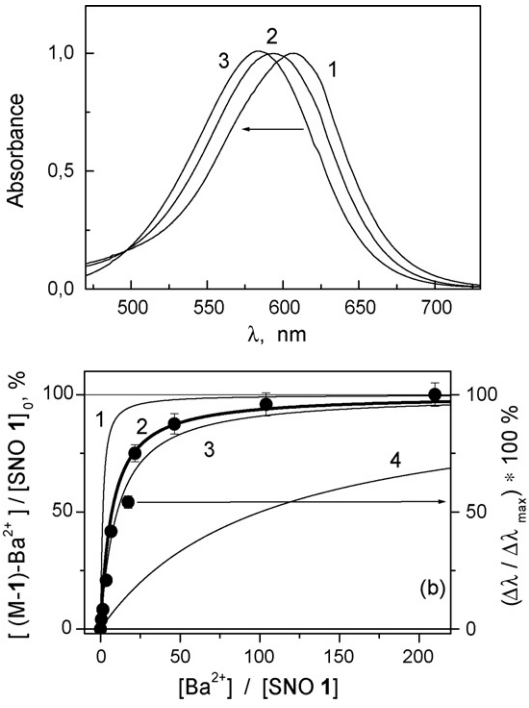

Fig. 9. Formation of complex between M-form of SNO **2** and Ba^{2+} ions in CH_3CN. (a) Hypsochromic shift of the M-form absorption band caused by addition of Ba^{2+}. Curves 1–3 denote to [Ba^{2+}]/[SNO **1**] = 0; 17; 104 correspondingly. Amplitudes of the bands are normalized to 1 in the maxima of M-form bands. (b) Determination of the equilibrium constants of the complex. Dots (right axis)—dependence of the shift of M-form absorption band maxima on the relative initial concentration of Ba^{2+} (M-form was obtained by the photolysis (366 nm, 298 K) in the cuvette box of spectrophotometer HP 8453). Solid lines (left axis)—calculation of the percent content of the complex. Curves 1–4 correspond to equilibrium constants 1×10^4; 1.5×10^3; 1×10^3; 1×10^2 M^{-1}.

For the crown-containing SNO **2** the stabilization effect (Table 1) could be explained by the same reason as for the case of SNO **1**, i.e. by the connecting of a cation to an oxygen atom of the merocyanine form of SNO complex with the metal cation. In the case of Mg^{2+}, the (M-**2**)-(Mg^{2+})$_2$ complex is formed (Scheme 3). The stability constant K_{12} = [(Mg^{2+})$_2$(S-**2**)]/[Mg^{2+}][Mg^{2+}(S-**2**)] was determined for (M-**2**)-(Mg^{2+})$_2$ (Table 2).

For the structure of Ba^{2+} complex with M-**2** two possibilities could be considered. When Ba^{2+} is added to (S-**2**)$_2$-Ba^{2+} complex to a large extent, one could expect either the conservation of the sandwich structure or the transition to the structure of (S-**2**)-Ba^{2+}. In the last case, Ba^{2+} cation should be situated above the crown-ether ring plane. Correspondingly, for the M-form one

could assume the formation of either a (M-**2**)-$(Ba^{2+})_2$ complex (as in the case of Mg^{2+}) or other structures.

4. Conclusions

In this paper, the formation of different complexes between SNO and rare earth metal cations is demonstrated. Complex formation changes the photochromic properties of spirooxazines and allows one to shift the range of M-form absorption up to 30 nm and to change the M-form lifetime up to an order of magnitude. This study could be considered as a necessary step in the development of photochromic systems with the controlled spectral and kinetic properties.

Acknowledgements

The work was supported by the Russian Foundation for Basic Research (grants No. 05-03-32474 and 05-03-32268), and the Program of Integration Projects of Siberian Branch of Russian Academy of Sciences (grant No. 77).

References

[1] H. Sasaki, A. Ueno, J.-I. Anzai, T. Osa, Bull. Chem. Soc. Jpn. 59 (1986) 1953.
[2] M. Inouye, M. Ueno, T. Kitao, K. Tsuchiya, J. Am. Chem. Soc. 112 (1990) 8977.
[3] M. Inouye, M. Ueno, K. Tsuchiya, N. Nakayama, T. Konishi, T. Kitao, J. Org. Chem. 57 (1992) 5377.
[4] K. Kimura, T. Yamashita, M. Yokoyama, J. Chem. Soc., Perkin Trans. 2 (1992) 613.
[5] K. Kimura, T. Yamashita, M. Yokoyama, Chem. Lett. (1991) 965.
[6] M. Tanaka, T. Ikeda, Q. Xu, H. Ando, Ya. Shibutani, M. Nakamura, H. Sakamoto, S. Yajima, K. Kimura, J. Org. Chem. 67 (2002) 2223.
[7] H. Sakamoto, H. Takagaki, M. Nakamura, K. Kimura, Anal. Chem. 77 (2005) 1999.
[8] Z. Liu, L. Jiang, Z. Liang, Y. Gao, J. Mol. Struct. 737 (2005) 267.
[9] Z. Liu, L. Jiang, Z. Liang, Y. Gao, Tetrahedron Lett. 46 (2005) 885.
[10] A.V. Chernyshev, N.A. Voloshin, I.M. Raskita, A.V. Metelitsa, V.I. Minkin, J. Photochem. Photobiol. A: Chem. 184 (2006) 289.
[11] K. Kimura, Y. Yamashita, M. Kaneshige, M. Yokoyama, J. Chem. Soc., Chem. Commun. (1992) 969.
[12] K. Kimura, M. Kaneshige, Y. Yamashita, M. Yokoyama, J. Org. Chem. 59 (1994) 1251.
[13] V.B. Nazarov, V.A. Soldatenkova, M.V. Alfimov, P. Larenzhini, A. Samat, R.R. Guglielmetti, Russ. Chem. Bull. 45 (1996) 1970.
[14] O.A. Fedorova, S.P. Gromov, Yu.P. Strokach, Yu.V. Pershina, S.A. Sergeev, V.A. Barachevskii, J. Pepe, A. Samat, R.R. Guglielmetti, M.V. Alfimov, Russ. Chem. Bull. 48 (1999) 1950.
[15] O.A. Fedorova, S.P. Gromov, Yu.A. Pershina, S.S. Sergeev, Yu.P. Strokach, V.A. Barachevsky, M.V. Alfimov, G. Pepe, A. Samat, R. Guglielmetti, J. Chem. Soc., Perkin Trans. 2 (2000) 563.
[16] O.A. Fedorova, Yu.P. Strokach, S.P. Gromov, A.V. Koshkin, T.M. Valova, M.V. Alfimov, A.V. Feofanov, I.S. Alaverdian, V.A. Lokshin, A. Samat, R. Guglielmetti, R.B. Girling, J.N. Moore, R.E. Hester, New J. Chem. 26 (2002) 1137.
[17] M.V. Alfimov, A.B. Balakin, S.P. Gromov, Yu.V. Zaushitsin, O.A. Fedorova, N.I. Koroteev, A.V. Pakulev, A.Yu. Resnyanski, A.P. Shkurinov, Zh. Fiz. Khim. 73 (1999) 1871 (in Russian).
[18] A.V. Feofanov, Yu.S. Alaverdian, S.P. Gromov, O.A. Fedorova, M.V. Alfimov, J. Mol. Struct. 563–564 (2001) 193.
[19] S. Minkovska, M. Fedieva, B. Jeliazkova, T. Deligeorgiev, Polyhedron 23 (2004) 3147.
[20] B.G. Jeliazkova, S. Minkovska, T. Deligeorgiev, J. Photochem. Photobiol., A: Chem. 171 (2005) 153.
[21] Yu.P. Strokach, T.M. Valova, V.A. Barachevskii, A.I. Shienok, V.A. Marevtsev, Russ. Chem. Bull. 54 (2005) 1477.
[22] Yu.V. Fedorov, O.A. Fedorova, S.P. Gromov, M.B. Bobrovskii, E.N. Andryukhina, M.V. Alfimov, Russ. Chem. Bull. 51 (2002) 789.
[23] Yu.V. Fedorov, O.A. Fedorova, E.N. Andryukhina, S.P. Gromov, M.V. Alfimov, L.G. Kuzmina, A.V. Churakov, J.A.K. Howard, J.-J. Aaron, New J. Chem. 27 (2003) 280.
[24] O.A. Fedorova, F. Maurel, E.N. Ushakov, V.B. Nazarov, S.P. Gromov, A.V. Chebunkova, A.V. Feofanov, I.S. Alaverdyan, M.V. Alfimov, F. Barigelletti, New J. Chem. 27 (2003) 1720.
[25] S.A. Ahmed, M. Tanaka, H. Ando, H. Iwamoto, K. Kimura, Tetrahedron 60 (2004) 3211.
[26] O.A. Fedorova, S.P. Gromov, M.V. Alfimov, Russ. Chem. Bull. 50 (2001) 1970.
[27] M.V. Alfimov, O.A. Fedorova, S.P. Gromov, J. Photochem. Photobiol. A: Chem. 158 (2003) 183.
[28] S. Kawauchi, H. Yoshida, N. Yamashina, M. Ohira, S. Saeda, M. Irie, Bull. Chem. Soc., Jpn. 63 (1990) 267.
[29] Yu.Yu. Lur'e, Spravochnik po Analiticheskoi Khimii (Handbook in Analytical Chemistry), Khimiya, Moscow, 1979, pp. 17–21 (in Russian).
[30] F. Arnaud-Neu, R. Delgado, S. Chaves, Pure Appl. Chem. 75 (2003) 71.
[31] S. Maeda, in: J.C. Crano, R. Guglielmetti (Eds.), Organic Photochromic and Thermochromic Compounds, Plenum Press, New York, 1999, pp. 86–109.
[32] Y.V. Shklyaev, Y.V. Nifontov, Heterocycl. Chem. (2003) 212.
[33] I.P. Pozdnyakov, V.F. Plyusnin, V.P. Grivin, D.Yu. Vorobyev, N.M. Bazhin, S. Pages, E. Vauthey, J. Photochem. Photobiol., A: Chem. 182 (2006) 75.
[34] M. Beck, I. Nagypal, Chemistry of Complex Equilibria, Academiai Kiado, Budapest, 1989, pp. 130–160.
[35] V. Lokshin, A. Samat, A.V. Metelitsa, Uspekhi Khimii 1971 (2002) 1015 (in Russian).